TRANSACTIONS OF THE INSTITUTE OF FLUID-FLOW MACHINERY

No. 133, 2016, 39–54

Łukasz Breńkacz*, Grzegorz Żywica

An experimental investigation conducted in order to determine bearing dynamic coefficients of two hydrodynamic bearings using impulse responses

Department of Turbine Dynamics and Diagnostics, Institute of Fluid Flow Machinery, Polish Academy of Sciences, 80-231 Gdańsk, Fiszera 14, Poland

Abstract

The paper presents the experimental investigation carried out in order to identify bearing dynamic coefficients of two hydrodynamic bearings from impulse responses. In this method the stiffness, damping and mass coefficients of two hydrodynamic bearings were calculated in a single algorithm. For each rotational speed, were obtained 12 dynamic coefficients which enable to fully describe the dynamic state of the rotor. Exciting force signals, applied using an impact hammer were shown. Displacements of the shaft were measured by eddy current sensors. The measurements were carried out at various rotational speeds, including resonance speeds. The vibration amplitude in a resonance case increases significantly with time after the excitation was induced by an impact hammer. Excitations of the rotor with an impact hammer were recorded using a high-speed camera. These unique recordings and simultaneous analysis of the trajectory of the bearing journals depict the contact phenomena that occur during impulse excitation of the rotor.

Keywords: Hydrodynamic bearings; Bearing dynamic coefficients; Experimental study

Nomenclature

d	–	rotor diameter
D	–	disc diameter

*Corresponding Author. Email adress: lbrenkacz@imp.gda.pl

l_1, l_2	–	distance of the disc to the first/second bearing support
l_{1p}, l_{2p}	–	displacement measurement points
L	–	bearing length
L_{shaft}	–	shaft length
$L_{teststand}$	–	test stand length
L_w	–	distance of a measuring point to the disc centre
P_1, P_2	–	measurement points
P_e	–	excitation point

1 Introduction

Values of stiffness and damping coefficients of hydrodynamic bearings are very important for vibration analyses carried out for fluid-flow machines [1,2]. Following difficulties found in the computational identification of such coefficients, many experimental methods for determination of their values have been proposed [3,4]. Experimental investigations were conducted with different types of bearings, in particular, with bearings that have a complex construction. The paper [5] presents the identification of dynamic coefficients of a hybrid gas bearing that has a sophisticated and robust construction with a complex structure of the foils. The bearing supports load both on a hydrostatic and hydrodynamic film. The Monte Carlo method was employed for the identification of dynamic parameters of a rotor supported by magnetorheological damping devices [6]. Literature studies showed that an experimental determination of stiffness and damping parameters of the bearings is conducted not only for radial bearings but also for thrust ones. The experimental identification of stiffness and damping characteristics for an axial foil bearing has been dealt with in detail in the article [7].

The method for the determination of bearing dynamic coefficients applied by the authors of this paper operates in frequency domain. Its first version was presented by Nordmann and Schoellhorn [8]. The basic algorithm was extended by adding the possibility to compute sixteen stiffness and damping coefficients [9].

The authors of the paper [10] modified the algorithm for the computation of stiffness and damping coefficients introduced by Qiu and Tieu in such a manner that it also allows calculating eight mass coefficients. The determination of stiffness, damping and mass coefficients by means of a single algorithm permits verification of the results already in a preliminary stage of an experimental investigation. The identified dynamic coefficients of a bearing can be verified on the basis of mass coefficients since a shaft mass is usually known in advance. This approach allows determination of all dynamical parameters of a rotor – bearings system by means of an experimental research.

The properly processed signal of a system response and an excitation force

signal are used to determine the values of bearings' dynamic coefficients in linear form. They are determined at specific operating conditions of the rotating system. The article [10] provides the example of calculations based on data from a numerical model. The part of a signal corresponding to the stable operation should be subtracted from the signal registered during the experimental testing [11]. The sensitivity of the method for identification of dynamic coefficients of hydrodynamic bearings based on a signal obtained from a numerical model is presented in [12]. The issues discussed in this paper included, inter alia, the impact of a nonuniform distribution of the force exciting rotor vibration, rotor unbalance, positioning of the measurement sensors, etc. It turned out that there are parameters which have a very significant impact on the results of experimental investigations, but some of them can be easily corrected.

The work described in this paper is a continuation of previously conducted research [10–13] in which the measurement method and its precision were described in detail. The article discusses the manner of performing experimental research. The construction of the test stand, the test apparatus used and the signals measured during experimental tests are covered. The video recordings taken by a high-speed camera demonstrate the impact hammer's slip over the surface of a rotating rotor shaft. The results of such testing have not yet been presented by any other researcher.

2 Basic technical characteristics of the test stand

The test stand for testing small rotors was built in order to conduct experimental research on rotor – bearings systems and to analyse defects, such as bearing damage, rotor unbalance, misalignment, etc. The photo of the test stand is presented in Fig. 1.

Figure 2 shows the diagram of the test stand on which the most important components are marked along with their dimensions. The length of the test stand is 1.25 m, and its width and height are 0.36 m and 0.65 m, respectively. The axes of the coordinate system used during the experimental investigation are shown in the top left-hand corner of this figure. The test stand rests on a 13 mm steel plate with attached two channel bars equipped with rubber feet that allow for height adjustment and leveling of the plate. Its weight – without the supporting structure – was approximately 60 kg. The rotor shaft was supported by two bearings. The system was driven by a three-phase motor with a maximum speed of 3450 rpm. The motor rotations were adjusted by means of a frequency inverter with a capacity of 1.5 kW. The motor was mounted to a gear that increases

Figure 1: Photo of the test stand.

the speed with a gear ratio 3.5:1. The presence of the inverter allows to vary the motor speed up to 12 000 rpm. The gear is connected to the rotor shaft by means of a permanent coupling. The coupling diameter is 50 mm and its length is 60 mm. The oil lubricated bearing system was equipped with the pump. During the experimental tests, the oil pressure was 0.16 MPa.

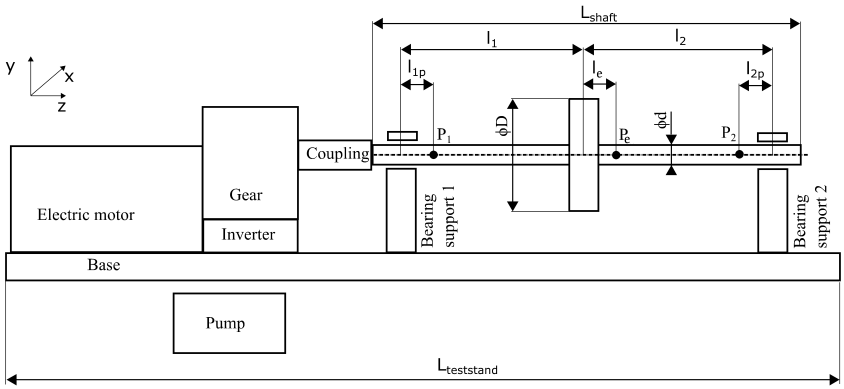

Figure 2: Diagram of the test stand.

The tested rotor had a length of $L_{shaft} = 920$ mm. The distance between the coupling and the first bearing support was 170 mm. The rotor was mounted in two bearing supports. The distance between the supports (i.e., $l_1 + l_2$) was

580 mm. The bearing located closer to the motor is marked with the number 1, while the bearing located on the other end of the rotor has the number 2. The rotor disc was precisely centered between the bearing supports, so the distances l_1 and l_2 equal each other (see Fig. 2). The rotor diameter was $d = 19.02$ mm and the rotor disc – $D = 152.4$ mm. The excitations were performed using an impact hammer at the point P_e, at a distance of $l_e = 30$ mm from the rotor disc's midpoint. For safety reasons, the rotor – bearings system was equipped with a lockable casing made of hard transparent plastic.

The rotor was supported by two hydrodynamic bearings with the same geometries. The radial bearing clearance was 76 μm and the bearing length was $L = 12.6$ mm. Every bearing had two supply ports situated on both sides of the shaft. The supply ports have a diameter of 2.54 mm. The viscosity grade of the lubricating oil was ISO 13.

3 Experimental testing procedure

The calculation diagram of the experimental determination of bearing dynamic coefficients is shown in Fig. 3. In the first step, the necessary research was carried out. The selected point P_e located on the rotor shaft surface (shown in Fig. 2) was hit in a horizontal direction (X) with an impact hammer when the rotor was operating at constant speed. This action was repeated around a dozen times within 40 s. Then, the measurement was repeated but hitting the shaft was realized in a vertical direction (Y). In the second step, the reference signal (corresponding to the stable operation of the rotor) was subtracted from the signal registered after the excitation. This operation was carried out using the computer program called 'Signal' [14], created for this purpose. The third step was zeroing values of the signal corresponding to an excitation force, omitting the values related to the main component. The signals thus obtained were subjected to a FFT (fast Fourier transform) analysis [15]. The spectral components received during the zeroing process are analyzed in a frequency domain. The matrixes **A**, **Z** and **I** were then created, the detailed description of which is given in the paper [10]. The dynamic coefficients of hydrodynamic bearings were calculated by the least squares method.

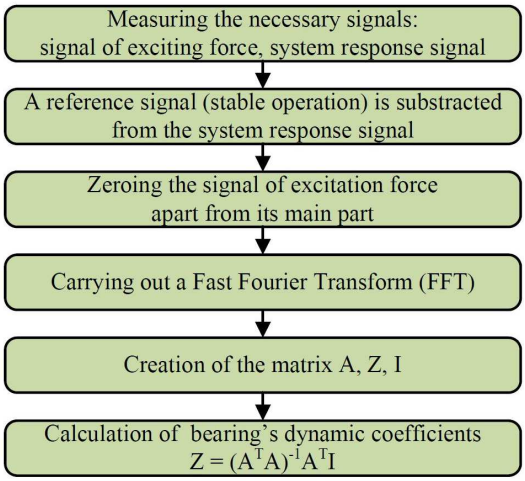

Figure 3: Calculation procedure for bearing dynamic coefficients.

4 Test apparatus

In fluid-flow machinery, unbalance and misalignment are common causes of elevated vibration levels [16]. Before starting the measurements, the shaft alignment was conducted by means of the OPTALIGN Smart RS device (manufactured by Prüftechnik) and two wireless laser sensors. The rotor was balanced using the Diamond 401 device, produced by MBJ Electronics s.c.

A SCADAS Mobile system, manufactured by LMS International, was used for data acquisition purposes. It was connected – via the Ethernet interface – to a laptop equipped with the Test.Lab 11B software. Four eddy current sensors (model CWY-DO-501A) were employed for measurements of the rotor displacement. The uniaxial displacement sensors were placed on the bearing supports. The eddy current sensors were positioned at the points P_1 and P_2 equidistant from the bearings ($l_{1p} = l_{2p} = 25$ mm). They were mounted at an angle of 90° to each other and at an angle of 45° to the axes of the global coordinate system. These sensors were connected to a SCADAS Mobile analyzer by means of a demodulator. Their maximum measurement range was 1 mm. Four uniaxial accelerometers (model 608A11) were implemented for vibration velocity measurements. The accelerometers were mounted in the bearing supports in two directions that were mutually perpendicular and also perpendicular to the rotational axis of the rotor. An impact hammer, 21.6 cm long and weights 0.16 kg – made by PCB Piezotronics – was employed to realize excitations. During the measurements, the hammer was fitted with a hard impact cap (ST STL), which implied that the

maximum impact force that could be obtained was 360 N. The rotational speed of the rotor was measured by using a 152 G7 laser tachometer, manufactured by Optel Thevon.

The analysis of a hammer impact in slow motion was also carried out within the framework of this research. A high-speed Phantom v2512 camera (manufactured by Vision Research) was employed for this purpose. The camera is equipped with a high-performance CMOS sensor and has a throughput of 25 Gpx/s which enables recording frames at 25 600 fps (frames per second) and 1280×800 pixels resolution. It enables recording frames at 1 million fps with the lowest resolutions and at 25 600 fps with the maximum resolution of 1280×800. For signal analysis, the software programs called PCC 2512 (Phantom Camera Control) and TEMA Motion were used, which were made by Vision Research and Image Systems, respectively. Two lenses were used, namely Zeiss Planar T* 50mm F/1.4 ZF.2 and Nikon 200 mm F4.0. ED-IF AF Micro-Nikkor.

5 Signal processing

In order to use the results from experimental research in further analysis, the signals must be processed in an appropriate way. The eddy current sensors are positioned at an angle of 45 ° to the axes of the global coordinate system. The appropriate processing of the signal registered for the first bearing was implemented by means of Eqs. (1) and (2). Analogical operations were carried out for the second bearing. The response recorded at the first bearing in the X direction after the excitation in the Y direction is denoted by 1XY. A transformed signal is denoted by 1XY'.

$$\begin{bmatrix} 1XX' \\ 1YX' \end{bmatrix} = \begin{bmatrix} \cos\emptyset & \sin\emptyset \\ -\sin\emptyset & \cos\emptyset \end{bmatrix} \begin{bmatrix} 1XX \\ 1YX \end{bmatrix}, \tag{1}$$

$$\begin{bmatrix} 1XY' \\ 1YY' \end{bmatrix} = \begin{bmatrix} \cos\emptyset & \sin\emptyset \\ -\sin\emptyset & \cos\emptyset \end{bmatrix} \begin{bmatrix} 1XY \\ 1YY \end{bmatrix}. \tag{2}$$

The signals registered by eddy current sensors were corrected using Eqs. (3) and (4). This correction was due to the fact that the sensors were situated next to the bearing supports, rather than at the bearing midpoints. Based on the sensitivity analysis described in article [12], it can be stated that the failure to take into account the above correction could have resulted in differences of several percentage points for the calculated values of bearing dynamic coefficients.

$$\begin{bmatrix} XX_1 & YY_1 \\ XX_1 & YY_2 \end{bmatrix} = \frac{1}{l_w + l_2} \cdot \begin{bmatrix} l_w + l_1 & l_w - l_1 \\ l_w - l_2 & l_w + l_2 \end{bmatrix} \begin{bmatrix} XX_{1p} & YY_{1p} \\ XX_{2p} & YY_{2p} \end{bmatrix}, \tag{3}$$

$$\begin{bmatrix} XY_1 & YX_1 \\ XY_1 & YX_2 \end{bmatrix} = \frac{1}{l_e + l_2} \cdot \begin{bmatrix} l_e + l_1 & l_w - l_1 \\ l_e - l_2 & l_e + l_2 \end{bmatrix} \begin{bmatrix} XY_{1p} & YX_{1p} \\ XY_{2p} & YX_{2p} \end{bmatrix} . \quad (4)$$

The calculations also reflect the fact that the point P_w (the point in which the excitation forces are acting) is not equidistant to both bearing supports, but has a distance of $l_w = 30$ mm to the rotor disc's midpoint. This fact has been taken into account by applying the necessary corrections using the formulas (5), (6) and (7).

$$l_{1f} = l_1 + l_e = 290 + 30 = 320 \text{ [mm]}, \quad (5)$$

$$l_{2f} = l_2 - l_e = 290 - 30 = 260 \text{ [mm]}, \quad (6)$$

$$F_{1shifted} = F_1 \frac{l_{2f}}{2l_1}, \quad F_{2shifted} = F_2 \frac{l_{1f}}{2l_2} . \quad (7)$$

6 Measurement results

If the shaft displacement signal at a bearing support is measured and recorded for 10 s (as shown in Fig. 4) it is possible to observe the 'rotor flow', besides the displacements related to the shaft revolutions that are changing 3250 times per minute. Such changes are specific to hydrodynamic bearings when the rotor shaft, apart from its rotational motion, also performs the motion in relation to the bearing bush. The vibration analysis is a very complex task in terms of spectral analysis, even for properly operating machines. In the vibration spectrum of a signal both harmonic (1X, 2X, 3X, ...) and sub-harmonic (X/2, X3, ...) components and also the components related to vibration of a supporting structure can be present.

In order to obtain a set of data required to determine bearing dynamic coefficients for a single rotational speed, a two-step analysis was necessary. In the first step the excitation force was applied in the Y direction (at the point P_w, see Fig. 2) by means of an impact hammer. In the second step, the measurement was conducted at the same rotational speed with the difference that hitting the shaft was realized in a horizontal direction (X). The exemplary signal of the excitation force acting in the Y direction was shown in Fig. 5a. Figure 5b presents the signal measured in the Y direction by an eddy current sensor positioned close to the bearing no. 2, when the rotor shaft was rotating at a constant speed of 4500 rpm. The graph shows a stable operation of the rotor together with periodic amplitude increases, caused by a hammer hit.

The values of the excitation force were around 80 N. The signal of the excitation force, shown for a shorter time period, is presented in Fig. 6. Most of the

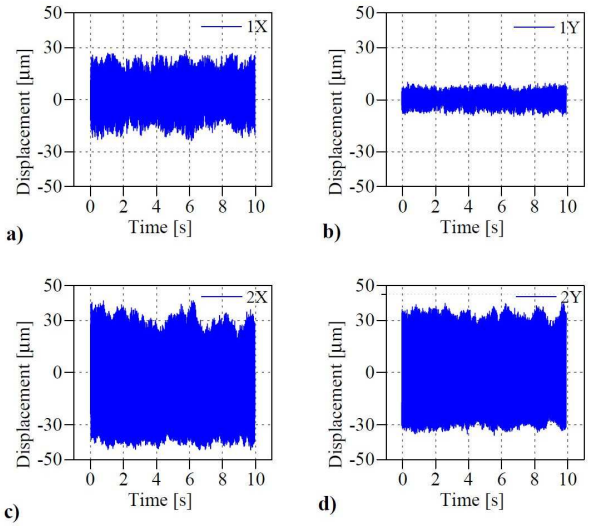

Figure 4: Stable operation of the bearing no. 1 (a and b) and no. 2 (c and d) at 3250 rpm. The graphs present the signals registered along the X (a and c) and Y (b and d) directions. The measurement time was 10 s.

excitations lasted from 0.1 ms to 0.2 ms. The values of the excitation force were zeroed, besides the values of the main peak. The exemplary results before and after zeroing these values can be seen in Figs. 6a and 6b, respectively.

Figure 7 contains the signal measured in the X and Y directions – Figs. 7a and 7b, respectively – during stable operation of the bearing no. 2. The next parts of this figure present the signals measured in the X and Y directions after applying the excitation in the X and Y directions – parts c) and d), respectively – by means of an impact hammer (the signal corresponding to this excitation force is shown in Fig. 6). It can be observed that the vibration amplitudes changed rapidly and then stabilized – the rotor returned to its stable operation. The amplitudes were increasing or decreasing (for a short period of time), depending on the present location of the rotor.

The computer program 'Signal' served to choose the relevant parts from the excitation forces and reference signals (i.e., the signals registered after the excitations). Choosing the appropriate signal ranges was the most time-consuming part of bearing dynamic coefficients calculation. The signals presented in Fig. 8 are the results of subtraction of the signals situated in Figs. 7a and7b from the signals visible in Figs. 7c and 7d, respectively. The left graph in Fig. 8 demonstrates the response signals corresponding to the bearing no. 1 after the excitation applied

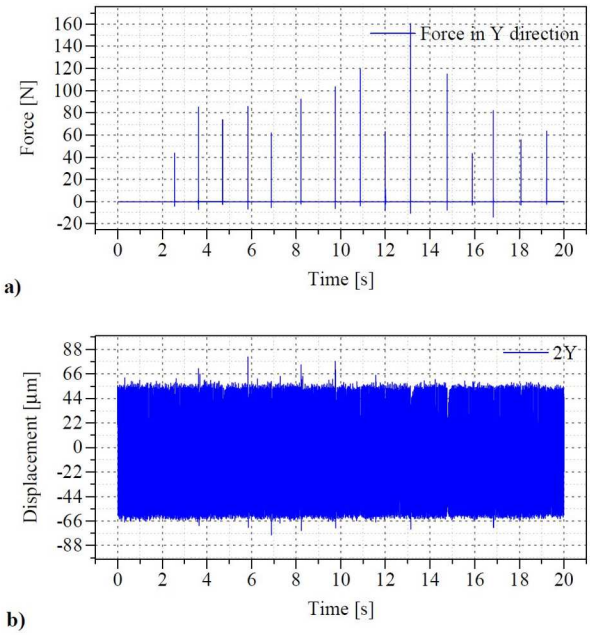

Figure 5: a) Excitation force vs. time. b) The signal measured in the Y direction close to the bearing no. 2 at 4500 rpm after the excitation in the Y direction was applied by an impact hammer.

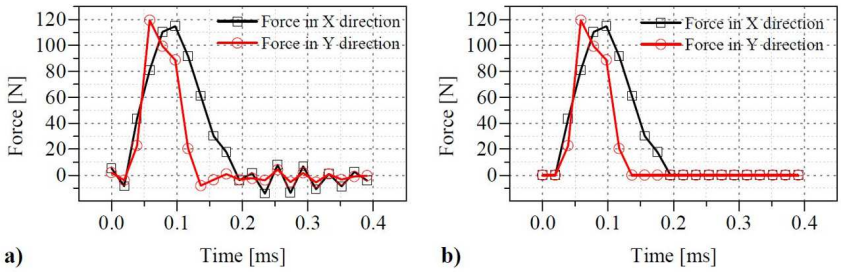

Figure 6: Excitation force in the X and Y directions vs. time. Excitations were applied at the speed of 4500 rpm: a) signal without zeroing values outside the range of the main component, b) signal with zeroing.

in Y (lines marked with 1YY and 1XY) and X (lines marked with 1YY and 1XY) directions. Similarly, the right graph in Fig. 8 shows the response signals which relate to the bearing no. 2. The first letter after the bearing number indicates the direction of displacement measurement and it is followed by the direction of

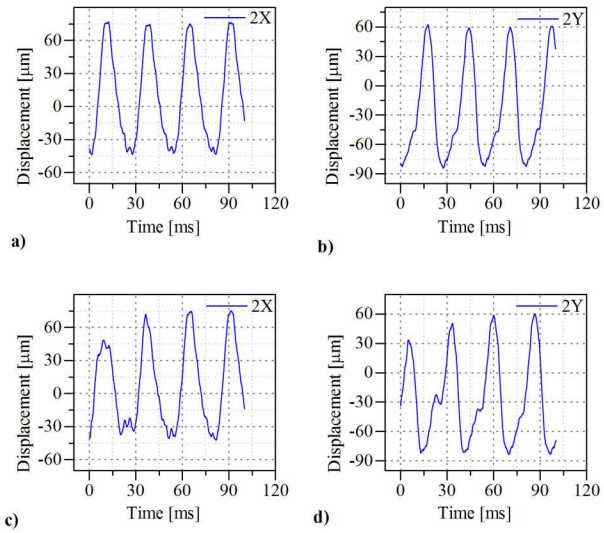

Figure 7: Stable operation of the bearing no. 2 at 4500 rpm (a and b) and the signal registered after applying the excitation (c and d). The graphs present the displacements in the X (a and c) and Y (b and d) directions.

excitation force. For instance, the system response signal registered in the X direction for the second bearing after the excitation force had been applied in the Y direction is indicated in Fig. 8b by means of the symbol 2XY.

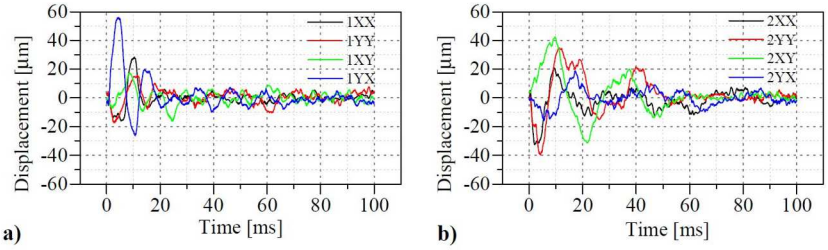

Figure 8: Vibration amplitude of the rotor after the excitation in X and Y directions vs. time: a) bearing no. 1, b) bearing no. 2 (the reference signal was subtracted from the signal obtained after excitation).

At some rotational speeds, vibration amplitudes have reached worryingly high levels that can be linked to the resonance phenomenon. Figure 9 demonstrates the signal registered at the second hydrodynamic bearing during its operation at a constant speed of 4000 rpm after the excitation in the Y direction was applied.

The signal registered before the excitation was subtracted from the signal recorded after the hammer strike was performed. It can be observed that the vibration amplitude rises from about 0 to above 30 μm within 0.3 s. Such behaviour is typical for systems functioning under unstable operating conditions and its occurrence can lead to machine damage.

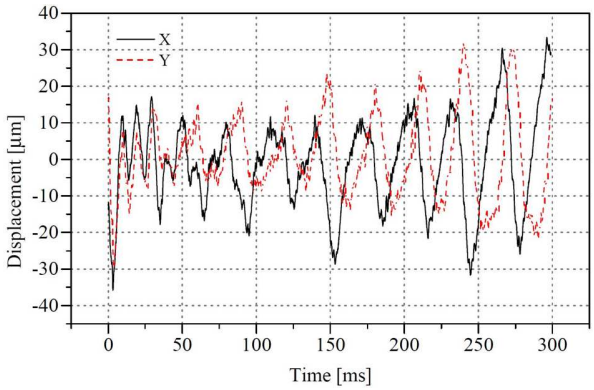

Figure 9: The vibration amplitude (that grows over time) registered on the bearing no. 2 at 4000 rpm after the excitation in the Y direction was applied by an impact hammer.

7 Analysis of the impact hammer slip

The way the impact hammer hits the rotor shaft is an important element of the research from the point of view of the accuracy of testing results. During numerical calculations, the effect of the hammer's slip over the surface of a rotating rotor shaft is extremely hard to implement in a computer program. Also, the possibility to observe this phenomenon during experimental tests is very difficult to achieve. The shaft displacements were registered (in two directions that were mutually perpendicular and also perpendicular to the rotational axis of the shaft) using the eddy current sensors situated next to the bearing supports. On this basis, it could not be concluded that the hammer strike was carried out as intended, i.e., in the specified direction of impact and without slipping. Therefore, it was decided to carry out observations using a high-speed camera.

Figure 10a shows one frame from a video recording in slow motion, showing the impact hammer's strike. The aluminium disc is visible on the left-hand side of this figure. A black-and-white striped ribbon was stuck on the rotor shaft in order to track its movement as precisely as possible. The impact hammer's cap is in the upper part of the figure. Figure 10b shows a zoomed-in shaft part in which

the excitations were applied by means of an impact hammer.

The duration of action of the exciting force (modal hammer contact with the shaft) is from 0.1 to 0.2 ms. The rotor diameter is 19.02 mm. The surface speed is 4489 mm/s at a shaft speed of 4500 rpm. The impact hammer surface can be regarded as a flat surface, the rotor surface is curved. After many hours of experimental research, there are visible slight traces of hits on the rotor surface. Their size does not exceed 0.5 mm. The duration of an impact is short enough that the friction force created after exciting through a modal hammer may be omitted. This fact was also confirmed by the observations made using a high-speed camera.

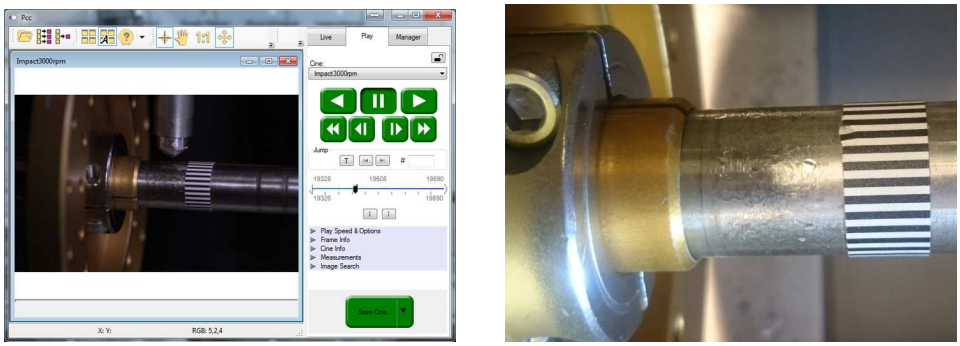

a) b)

Figure 10: a) Recording made with a high-speed camera. The only frame visible shows the impact hammer's cap. b) Rotor shaft on the surface of which are visible traces of hits.

The description of the hammer movement recorded by means of a high-speed camera is quite cumbersome. However, the experimental investigation has shown that the hammer slip is small and may be neglected. Forces that act on the rotor may be treated as excitations applied in the directions corresponding to a direction of one of the axes (X or Y). This information is valuable and confirms the relevance of initial assumptions made.

8 Summary and conclusions

The article presents the experimental research aiming at the determination of stiffness, damping and mass coefficients of two hydrodynamic bearings. The associated methodology employed has been described in detail, including measured signals and their processing required for carrying out the calculation process.

Moreover, the tests were also performed by means of a high-speed camera.

The paper available in the scientific literature describe various algorithms for estimation of bearing dynamic coefficients. It is very rare to encounter paper giving a detailed description of signals measured experimentally. However, there are many paper describing the impulse method for determining the parameters of bearings, seals and dampers [17,18]. The lack of thorough analyses concerning the excitation response signals and their processing in the current literature were the motive for writing this article. Another novelty in this paper is the consideration given on the impact hammer slip.

The experimental studies involved the measurement of the forty seconds periods of rotor operation (around a dozen times) during which the rotor vibrations were excited using an impact hammer hitting the shaft separately in two perpendicular directions. Only the signal fragments beginning with the moment of impact and ending after the time the rotor returns to the normal operation were used as the basis for calculations. The computer program called 'Signal' has proven to be an effective tool for selecting signals, their processing and storing in a suitable form.

The signal preparation procedure included the subtraction of the reference signal (i.e., the signal registered just before the excitation occurred) from the signal measured immediately after the excitation took place. Such a procedure was carried out for two bearings in a single operation and for every excitation signal that was measured by eddy current sensors. In general, it may be said that finding the reference signals was relatively easy for the entire speed range. However, in the case of some speeds near the resonance speed (around the speed of 4000 rpm), this task was slightly more difficult, mainly due to the fact that the registered signals were phase-shifted – it was detected after comparison of the frequency of a sinusoidal signal measured by the eddy current sensor situated next to the bearing support no. 1 with the frequency of the signal measured in the same direction by the sensor positioned close to the bearing support no. 2.

It seemed that the impact hammer's slip (and the related unequal distribution of exciting forces on the rotor shaft surface) occurring during the experimental tests is a factor which may have an impact on calculation results. The contact of the hammer with a fast-rotating shaft surface may result in the situation that the excitation force is not perpendicular to the axis of the shaft. No information is available on this point in the scientific literature. The numerical computations performed also did not allow for verification of whether a slip of the impact hammer can have a considerable impact on the results obtained. The authors of the article came up with the idea of using a high-speed camera in order to study this

phenomenon in a slow motion. The observation of the impact hammer's strike (using the 1/250th slow motion playback mode) has led to the conclusion that the contact time is sufficiently short to assume that the direction of force applied by the hammer is fully in line with the intended direction.

Acknowledgement The research is financed by the Polish National Science Centre as a research project no. 2015/17/N/ST8/01825.

Received in July 2016

References

[1] Kiciński J. and Żywica G.: *Steam Microturbines in Distributed Cogeneration*. Springer, 2014.

[2] Kiciński J.: *The Dynamics of Rotors and Slide Bearings*. IMP PAN, Maszyny Przepływowe, Gdańsk 2005 (in Polish).

[3] Dimond T.W., Sheth P.N., Allaire P.E., He M.: *Identification methods and test results for tilting pad and fixed geometry journal bearing dynamic coefficients – A review*. Shock Vib. **16**(2009), 1, 13–43.

[4] Tiwari R., Lees A.W., Friswell M.I.: *Identification of dynamic bearing parameters: a review*. Shock Vibrat. Digest. **36**(2004), 2, 99–124.

[5] Delgado A.: *Experimental identification of dynamic force coefficients for a 110 mm compliantly damped hybrid gas bearing*. J. Eng. Gas Turb. Power **137**(2015), 7, 072502-072502-8.

[6] Zapomel J., Ferfecki P., and Kozánek J.: *Application of the Monte Carlo method for investigation of dynamical parameters of rotors supported by magnetorheological squeeze film damping devices*. Appl. Computat. Mech. **8**(2014), 129–138.

[7] Arora V., Van der Hoogt P.J.M., Aarts R.G.K.M., De Boer A.: *Identification of stiffness and damping characteristics of axial air-foil bearings*. Int. J. Mech. Mater Des. **7**(2011), 3, 231–243.

[8] Nordmann R., Schoellhorn K.: *Identification of stiffness and damping coefficients of journal bearings by means of the impact method*. In: Proc. 2nd Int. Conf. on Vibrations in Rotating Machinery, 1980, 231–238.

[9] Qiu Z.L., Tieu A.K.: *Identification of sixteen force coefficients of two journal bearings from impulse responses*. Wear **212**(1997), 2, 206–212.

[10] Breńkacz Ł.: *Identification of stiffness, damping and mass coefficients of rotor – bearing system using impulse response method*. J. Vibroeng. **17**(2015), 5, 2272–2282.

[11] Breńkacz Ł.: *Identification of bearing dynamic coefficients with consideration of shaft unbalance*. Mechanik **7**(2015) (in Polish).

[12] Breńkacz Ł., Żywica G.: *The sensitivity analysis of the method for identification of the bearing dynamic coefficients*. Springer Proc. Dyn. Sys. – Modeling (2016) (accepted for printing).

[13] Breńkacz Ł., Żywica G.: *Numerical estimation of linear and nonlinear stiffness and damping coefficients of journal hydrodynamic bearings*. Mechanik **7**(2016), 648–649, (in Polish).

[14] Breńkacz Ł.: *Adequacy ranges of linear and nonlinear methods for determining the dynamic properties of the rotating machinery*. Doctoral dissertation, Gdańsk 2016 (in Polish).

[15] Rao K.R., Kim D.N., Hwang J.J.: *Fast Fourier Transform – Algorithms and Applications*. Dordrecht 2010.

[16] Muszyńska A.: *Rotordynamics*. Taylor & Francis, LLC, Boca Raton 2005.

[17] Manikandan S., Tiwari R., Dwivedy S.K.: *Identification of rotor dynamic parameters of seals using impact hammer method*. In: Proc. 12th Nat. Conf. on Machines and Mechanisms (NaCoMM-2005), IIT Guwahati, Dec. 16–17, 2005, 384–390.

[18] Lal M., Tiwari R.: *Multi-fault identification in simple rotor-bearing-coupling systems based on forced response measurements*. Mech. Mach. Theory **51**(2012), 87–109.